ELSEVIER

Biophysical Chemistry 125 (2007) 92 – 103

Biophysical Chemistry

http://www.elsevier.com/locate/biophyschem

EPR spectroscopy and theoretical study of γ-irradiated asparagine and aspartic acid in solid state

Grazyna Strzelczak [a], Jacqueline Bergès [b,*], Chantal Houée-Levin [c], Dariusz Pogocki [a,d], Krzysztof Bobrowski [a]

[a] *Institute of Nuclear Chemistry and Technology, 03-195 Warsaw, Poland*
[b] *LCT, UMR 7616, Université Pierre et Marie Curie, 4 place Jussieu 75230 Paris cedex 5, France*
[c] *LCP, UMR 8000, Bldg 350, F-91405 Orsay, France*
[d] *Rzeszow University of Technology, Faculty of Chemistry, Department of Biochemistry and Biotechnology, 6 Powstancow Warszawy Ave. 35-959 Rzeszow, Poland*

Received 11 May 2006; received in revised form 29 June 2006; accepted 30 June 2006
Available online 11 July 2006

Abstract

Aspartic acid (Asp) and asparagine (Asn) are vulnerable amino acids. One-electron addition or withdrawal reactions initiate many deleterious processes involving these amino acids. To study these redox processes we have irradiated by γ-rays asparagine or aspartic acid in the solid state. The nature of the resulting free radicals was determined by electron paramagnetic resonance (EPR) and by calculations using DFT methods in various environments. Reactions initiated by electron transfer are different for both amino acids: Asn anion loses hydrogen atom whereas the cation undergoes decarboxylation. Conversely, Asp cation loses hydrogen atom from amine group, which triggers decarboxylation.

Keywords: Asparagine; Aspartic acid; Electron paramagnetic resonance (EPR); γ-Radiolysis; DFT calculations

1. Introduction

Aspartic acid (Asp) and asparagine (Asn) residues (Chart 1) are important in several processes. For instance, Asp is a specific cleavage site for caspases and thus is a key residue in apoptosis processes [1]. As for Asn, it is the site of N-glycosylation leading to N-linked glycosaccharides. This reaction, which occurs on the surface of protein, is essential for numerous processes involving protein recognition [2]. N-glycosylation has a stabilizing effect on the protein structure and increases the resistance to denaturation or proteolysis.

The well-known deamidation of Asn and Gln, was documented because of its occurrence in all tissues [3]. Oxidative damage enhances asparagine instability [4] which indicates a free radical route in asparagine degradation. In conditions of oxidative stress, aspartic acid is also modified. It leads to isoaspartic acid [5]. Peptide bond cleavage at Asn associated with aging was also reported [6]. It results in triggering of protein degradation. Similarly one-electron oxidation in lysozymes leads to cleavage at Asn [7]. Age-related oxidative stress induces also changes in proteins among which results in enhancement of Asn-Asp instability [4]. Asn is a highly conserved amino acid in the family of cyclooxygenases, key enzymes in inflammation processes [8]. Since these enzymes function in conditions of oxidative stress, the behaviour of Asn residue toward free radicals is important. Even if they do not belong to the active site, these residues are important in maintaining the three dimensional structure of proteins by their participation in hydrogen bond network [9].

In the gas phase, within mass spectrometry experiments, sequences Gln-Gly are a dissociation site [10]. Peptides containing asparagine residues undergo side chain cleavages during dissociative electron attachment and it was proposed that

* Corresponding author. LCT, UMR 7616, Casier 137, Université Pierre et Marie Curie, 4 place Jussieu 75230 Paris cedex 5, France. Tel.: +33 1 44 27 9659; fax: +33 1 44 27 4117.
E-mail addresses: grazyna@ichtj.waw.pl (G. Strzelczak), jb@lct.jussieu.fr (J. Bergès), chantal.houee-levin@lcp.u-psud.fr (C. Houée-Levin), kris@ichtj.waw.pl (K. Bobrowski).

0301-4622/$ - see front matter © 2006 Elsevier B.V. All rights reserved.
doi:10.1016/j.bpc.2006.06.017

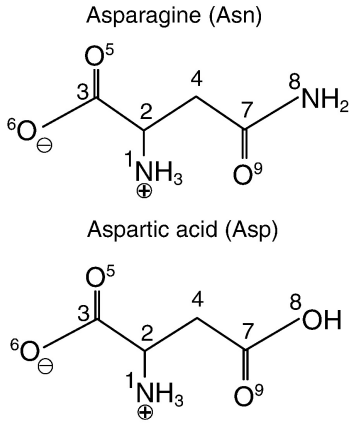

Chart 1.

such losses could be used to ascertain the presence of this residue in unknown peptides [11]. As far as radiosterilization of food and drugs is concerned, one should be able to predict the radiation-induced modification in the solid state. Irradiation of proteins in the solid state, either lyophilised or in frozen aqueous solution, induces peptide bond breakage leading to non-random fragmentations [12]. It was shown that sequences containing asparagine or aspartate residues are prone to peptide bond cleavage leaving these residues either as a C-terminal or as a N-terminal. These processes are poorly understood despite their importance in many biological (radioprotection, radiotherapy) and industrial processes (radiosterilization of food and drugs).

To the best of our knowledge there is no many reports about mechanisms of radiation damage of L-aspartic acid and L-asparagine. Characterization of radicals derived from them has never been performed in the same conditions by the same author. Moreover, due to the complexity of the EPR spectra and the lack of the appropriate software identification of radicals has not been attempted [13]. In the present work we wish to report comparative studies on dominant radicals which are formed in L-aspartic acid and L-asparagine in solid state after γ-irradiation. In spite of differences in structures limited to their side chains (amide group vs. carboxyl group) one can expect formation of the same type of radicals resulting from decarboxylation, deamination, deamidation or hydrogen abstraction. Therefore, comparison of EPR spectral features observed in both amino acids should be of a great help in elucidation of radical transformation mechanisms induced by radiation.

Free radicals were detected and characterized by EPR spectroscopy at various temperatures and CO_2 was detected and quantified by gas chromatography. Mechanisms leading to their appearance are proposed based on calculations by DFT methods.

2. Experimental

L-Asparagine and L-aspartic acid were purchased from Sigma-Aldrich Chemie GmbH, Germany. These compounds were of the highest commercially available grade of purity.

The samples of powdered Asn and Asp were evacuated and irradiated in liquid nitrogen with the dose of 4 kGy in ^{60}Co-γ-source (Issledovatiel, USSR). The radicals produced by radiation were studied over the temperature range of 77–293 K by applying electron spin resonance (ESR) technique using a Bruker ESP-300 spectrometer operating in the X-band (9.5 GHz) equipped with a variable temperature unit. The EPR spectra were recorded at various microwave power (1–40 mW) and modulation amplitude (0.01–0.5 mT). The optimized experimental parameters were: 1 mW (microwave power) and 0.1 mT (modulation amplitude).

The ESR spectra were analyzed by the computer simulation program PEST WinSIM [14]. This program adjusts the values of the simulations parameters to create the best fit between simulated and experimental spectra. In spite of the fact that this program was designed to compute the simulations of multiple species of isotropic EPR spectra, its application is justified for powdered samples. Due to the many possible orientations of the radicals in the magnetic field, the X-band EPR spectra of the powdered samples are given by broad lines. Therefore, anisotropic features of spectra are not visible.

Carbon dioxide analysis was performed by means of the gas chromatographic head-space technique using a Shimadzu GC-14C gas chromatograph equipped with a thermal conductivity detector and a Porapak Q column.

3. Computational details

All geometries of the isolated species were optimized using a gradient technique. Calculations were performed with the standard basis sets (6-31G*) for the DFT (B3LYP) method using the programs Gaussian 98 and 03 [15]. The use of this relatively small basis set is justified by the number of geometry optimizations that had to be performed, and by the fact that DFT methods are known to be slightly dependent on the basis set [16]. Moreover, our previous works demonstrated that such basis sets are sufficient [17–19]. This method is commonly used for localised radical structures [20]. For bound systems reasonable estimates of electron affinities can be obtained with DFT theory [21]. The influence of environment on neutral and charged radicals was taken into account by adopting Polarised Continuum Models (PCM) with the COSMO option for the Polarised Continuum Model CPCM [22,23]. Electrostatic and non-electrostatic terms are included in the CPCM values. While computational results are probably accurate within 4–8 kJ mol^{-1} in vacuum, the errors in the liquid phase are still difficult to be estimated [24]. Bond dissociation energies (BDE) were calculated as the difference between the computed total energies of products (radicals obtained after bond breaking) and reactants (parent molecules). Zero point energy corrections were found very small. Calculations of hyperfine constant splittings (a_H) were carried out using both bases sets: the standard one and the well adapted EPR-III [25]. The geometries of solvated species were reoptimized by both methods.

4. Results

A detailed analysis of EPR experimental data and theoretical calculations using DFT allows elaboration of the mechanism of Asp and Asn degradation induced either by ionization or by an attachment of electron.

4.1. Asparagine

4.1.1. Experimental EPR results

In asparagine at 77 K, a broad doublet is observed with $g=2.003$ and a hyperfine splitting $a=24$ G (Fig. 1, top). Similar doublets were detected at 77 K in various amino acids and were assigned to radical anions formed upon addition of an electron. Therefore, the doublet is attributed to the asparagine radical anion, in agreement with Sevilla who observed a broad doublet with a similar splitting in asparagine [26]. The localization of the excess electron is presumed to be either on the carboxyl group [27,28] or on the amide function [26]. At 160 K, a pure doublet of doublets was observed with spectroscopic hyperfine splittings of $a_{H\alpha}=15$ G and $a_{H\beta}=3.5$ G and $g=2.003$ (Fig. 1, middle). This signal is attributed to the hydrogen abstraction radical from the methylene group in the side chain of asparagine. The same type of radical has been identified previously by Close et al. in a single crystal of asparagine [29] at room temperature. However, its experimental spectroscopic hyperfine splitting $a_{H\alpha}$ extracted from the complex EPR spectrum is different ($a_{H\alpha}=22$ G). On further warming to about 250 K, additional signal was observed. This new multiline signal was resolved into two components: the doublet of doublets previously observed and a four line component with $a_{H\alpha}=21$ G and $a_{H\beta}=23$ G. The latter component was assigned to the decarboxylated asparagine radical. As the temperature was increased to 273 K, the spectrum in asparagine indicated the presence of three radical species (Fig. 1, bottom). The experimental spectrum stable at room temperature (Fig. 2A) can be simulated (Fig. 2A) by a previously recorded at lower temperatures four-line component with $a_{H\alpha}=21$ G and $a_{H\beta}=23$ G (Fig. 2B) (20%), a doublet of doublets with $a_{H\alpha}=15$ G and $a_{H\beta}=3.5$ G (Fig. 2C) (40%) and by a new wide multiline component with $a_{H\alpha}=22$ G and $a_{H\beta}=42$ G (Fig. 2D) (40%). The multiline component was assigned to asparagine deamidated radicals.

4.1.2. Theoretical results

Asparagine and aspartic acid are zwiterrionic in the crystal environment. Since it was not possible to consider either the whole crystal or the zwitterion in the vacuum, we mimicked the crystal environment by two media with different dielectric constants: water ($\varepsilon=78$) and ethanol ($\varepsilon=24$), that stabilize zwitterions. Additional calculations were performed with $\varepsilon=2$ (CCl_4) in which zwitterions are less stabilized. We compare the results with those obtained in vacuum.

Energies are reported in Table 1, BDE in Table 2 and Charges in Table 3. Coupling constants ($a_{H\alpha}$) calculated theoretically are summarised in Table 4 along with the respective spin densities. They were calculated from optimized geometries in the vacuum, in water and in ethanol. The optimization and a_H calculations were also performed for zwitterions in water with EPR-III basis.

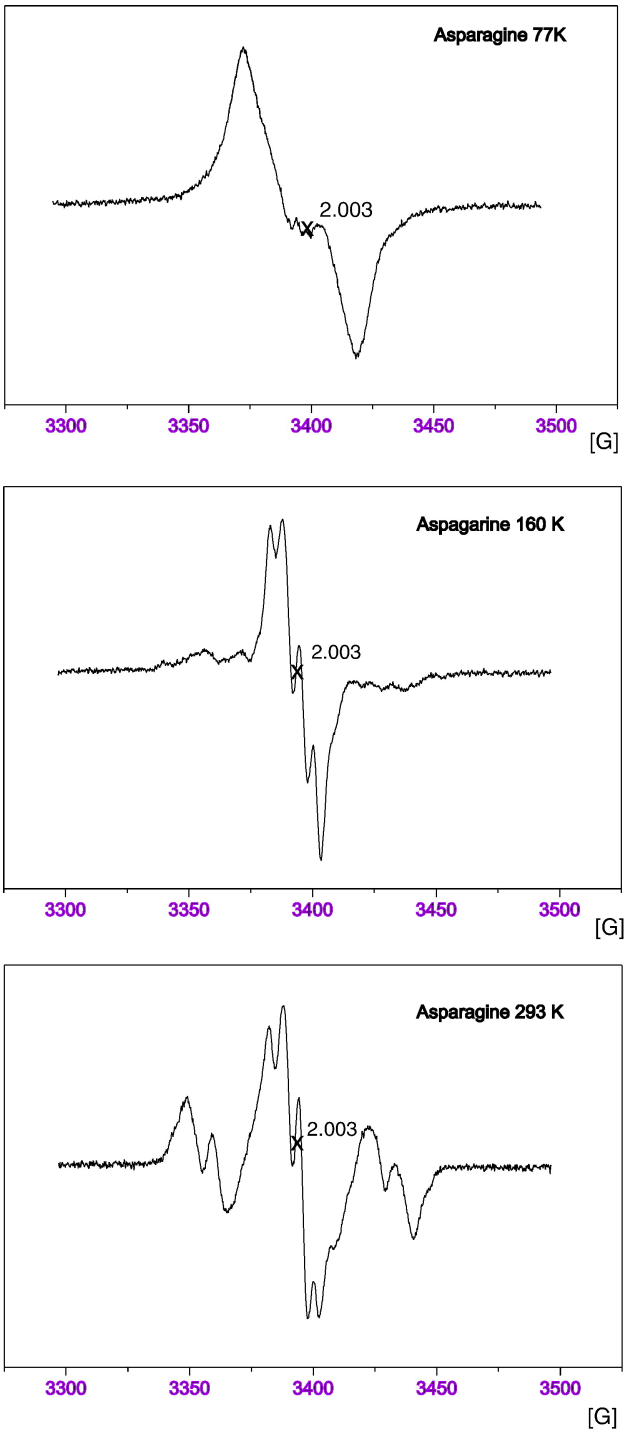

Fig. 1. Experimental EPR spectra recorded at 77 K (top), 160 K (middle), and 293 K (bottom) in asparagine irradiated at 77 K.

4.2. Structures, energies and charge distributions

Two stable conformations were obtained named respectively Asn1 and Asn2. Asn1 is stabilized by an intramolecular

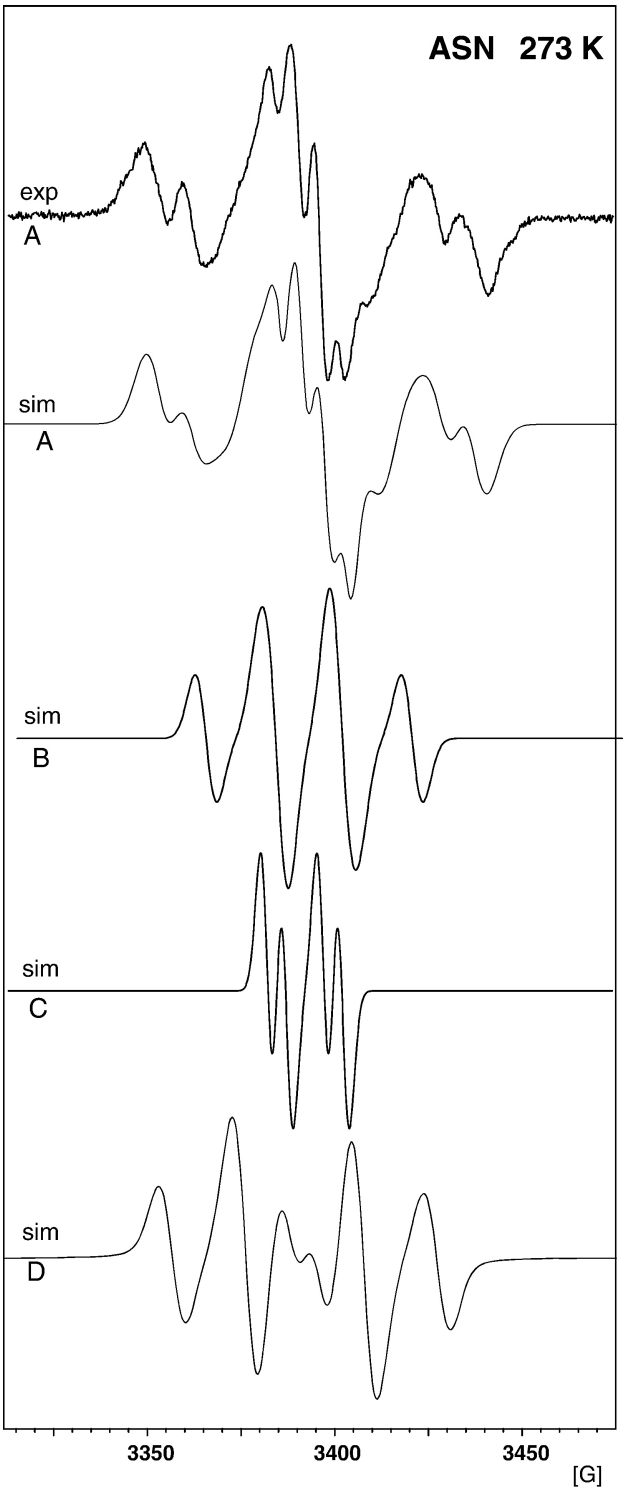

Fig. 2. Experimental and simulated multicomponent spectrum recorded at 273 K in asparagine irradiated at 77 K (A). Simulated spectrum consists of 20% of a quartet (B), 40% of doublet of doublets (C), and 40% of multiline component (D). See text for assignments and hyperfine splittings.

hydrogen bond between $-NH_2$ of amide and the carboxylate function (Fig. 3, structure a). This hydrogen bond does not exist in Asn2 and as a consequence this form has a higher energy (Table 1). Asn2 structure is very close to the experimental one obtained by neutron diffraction on crystal [30,31]. Radical anions and radical cations were fully optimized starting from both conformations.

Table 1
Energies of Asparagine and radicals derived from Asn

Environment →	Zwitterions in water (ε=78)	Zwitterions in ethanol (ε=24)	Vacuum
Entity ↓	*E* (a.u.)	*E* (a.u.)	*E* (a.u.)
Asn	−492.47243	−492.46071	−492.43052
	−492.47092		
Asn radical cation	−492.25515	−492.22764	
Asn radical cation deprotonated	−491.81013	−491.78973	−492.13318
Asn radical anion	−492.54008	−492.44322	−492.40416
Asn without H on C2	−491.81177	−491.80191	−491.81375
Asn without H on C4	−491.81643	−491.81005	−491.77416
H	−0.49790	−0.498611	−0.50027
H_2	−1.17561	−1.17560	−1.17548
Decarboxylated Asn	−303.68267	−303.67571	−303.21140
CO_2	−188.58030	−188.58451	−188.58094
Deamidated Asn	−323.09019	−323.08204	−323.06376
$CONH_2$	−169.24357	−169.24580	−169.23206

The radical anion is unstable and loses hydrogen atom from the amine group (Fig. 3, structure c). As far as radical cations derived from Asn1 are concerned they could not be optimized because they underwent loss of CO_2: C2–C3 bond (Chart 1) elongated and the O5–C3–O6–angle changed to 180°, whereas in those derived from Asn2, optimization leads to a stable structure with the same C2–C3 bond elongated. It is interesting to note that the C4–C7 bond does not change significantly upon oxidation (Fig. 3, structure b).

Moreover, the loss or addition of one electron leads to similar conformations with simultaneous breaking of the hydrogen bond (Fig. 3, structures b and c). We have also considered the possibility of deprotonation of the amine function in radical cation. Within this assumption, it was possible to get the optimized deprotonated radical cation. Similar structural changes are observed as far as the respective bond lengths (C2–C3 and C4–C7) are concerned. These data suggest that electron ejection that leads to both protonated and deprotonated forms of radical cations is followed by the fragmentation mainly via decarboxylation pathway with a

Table 2
Bond dissociation energies in asparagine (Asn) and aspartic acid (Asp)

Environment →	Zwitterions in water (ε=78)	Zwitterions in ethanol (ε=24)	Vacuum
Bond ↓	*E* (kJ mol^{-1})	*E* (kJ mol^{-})	*E* (kJ mol^{-1})
Asparagine			
C2–C3 (decarboxylation)	549.4	525.8	361.7
C4–C7 (deamidation)	363.7	348.5	353.3
C2–H (H abstraction)	426.9	420.1	305.5
C4–H (H abstraction)	414.6	398.8	409.4
Aspartic acid			
C2–C3 (decarboxylation)	553.4	534.0	360.1
C4–C7 (decarboxylation)	554.0	522.8	402.6
C2–H (H abstraction)	459.8	421.4	314.3
C4–H (H abstraction)	423.3	407.8	401.5

Table 3
Mulliken charge distribution in parent molecules (zwitterions in water) and in radicals derived

Asparagine								
Atom	Asn	Radical anion	Radical cation, $-NH_3^+$	Radical cation NH_2	Asn C2(–H)	Asn C4(–H)	Asn ($-CO_2$)	Asn ($-CONH_2$)
N_1	0.59	**−0.14**	0.64	**−0.09**	0.55	0.60	0.66	0.54
C_2	0.14	0.08	0.20	0.15	0.17	0.11	0.25	0.17
C_3	0.59	0.49	0.64	0.61	0.58	0.59		0.57
O_5	−0.64	−0.67	**−0.36**	**−0.36**	−0.65	−0.62		−0.65
O_6	−0.65	−0.71	**−0.52**	**−0.52**	−0.66	−0.63		−0.66
C_7	0.57	0.57	0.65	0.62	0.57	0.56	0.59	
N_8	−0.03	−0.04	0.09	0.06	−0.08	−0.06	0.66	
O_9	−0.59	−0.56	**−0.44**	**−0.48**	−0.56	−0.59	−0.56	

Aspartic acid								
Atom	Asp	Radical anion	Radical cation, $-NH_3^+$	Radical cation, NH_2	Asp C2(–H)	Asp C4(–H)	Asp ($-CO_2$)	Asp ($-CO_2$)
N_1	0.58	**0.46**		**0.13**	0.53	0.55	0.64	0.64
C_2	0.14	0.12		0.19	0.19	0.10	0.27	0.20
C_3	0.58	0.55		0.61	0.57	0.60		0.63
O_5	−0.66	−0.66		**−0.48**	−0.66	−0.63		−0.49
O_6	−0.66	−0.67		**−0.49**	−0.68	−0.64		−0.08
C_7	0.59	0.56		0.62	0.62	0.58	0.61	
O_8	−0.11	**−0.32**		−0.11	−0.11	−0.11	−0.11	
O_9	−0.51	**−0.71**		−0.53	−0.49	−0.52	−0.50	

In bold, major changes in radicals compared to the parent molecule.

small contribution, if any, of deamidation pathway. The respective energies of radical cations and radical anions calculated for various environments are reported in Table 1. The respective ionization potentials vary with medium (5.9, 6.3, 7.3 and 8 eV in water, ethanol, CCl_4 and vacuum, respectively).

We have also considered hydrogen atom abstraction from both C2 and C4 atoms. Both abstraction processes result in alkyl radicals quasi isoenergetic (Table 1) and with very similar structures (Fig. 3, structures d and e). Taking the respective energies into account BDEs of C2–H and C4–H bonds were calculated (Table 2). They are not much sensitive to the environment and hydrogen abstracted (ranged from 400 to 430 kJ mol^{-1}) except for hydrogen abstraction from C2 (305 kJ mol^{-1}) in the vacuum. In fact, the stabilizing effect of zwitterionic form does not exist in vacuum.

The free radicals resulting from decarboxylation and deamidation were optimized and their stable structures were obtained. The respective energies of these radicals calculated for various environments are reported in Table 1. Taking these energies into account, BDEs of the C2–C3 bond (associated with decarboxylation) and the C4–C7 bond (associated with deamidation) were calculated (Table 2). Generally, BDEs are higher for the C2–C3 bond in comparison to the C4–C7 bond (e.g. 549 kJ mol^{-1} vs. 364 kJ mol^{-1} in water).

Mulliken charge distributions are presented in Table 3. Changes in the negative charge distribution after oxidation involve mainly oxygen atoms in carboxyl and amide groups. One has to note that positive charge distribution on the nitrogen atom located in the amine group N1 is almost not affected. However, for the deprotonated radical cation, N1 atom becomes negatively charged due to a loss of proton. For the radical anion a change in charge distribution takes place mainly on the nitrogen atom N1 due to a loss of hydrogen atom (see Fig. 3, structure c). It is interesting to note that charge distribution in hydrogen abstraction radicals remains almost the same in comparison to the parent molecule.

4.2.1. Coupling constants and spin densities

A fairly good agreement was found between experimentally measured and calculated $a_{H\alpha}$ values for decarboxylation and deamidation radicals derived from asparagine in zwitterionic forms (in water, ethanol and CCl_4) (Table 4). Discrepancy noted between experimentally measured and calculated $a_{H\alpha}$ values for decarboxylation radicals in vacuum confirms also that the amine group in these radicals is protonated. As far as H-abstraction radicals from the carbon atom C4 are concerned, the calculated $a_{H\alpha}$ values are higher from those observed experimentally.

In water, ethanol and CCl_4, in the radical cation and its deprotonated form, a spin density is distributed on the oxygen atoms located in both carboxylate and amide functionalities. A spin density is additionally spread over the nitrogen atom located in the amine group in deprotonated form of the radical cation in the vacuum. In H-abstraction radicals, deamidation and decarboxylation radicals spin density is mainly located on the respective carbon atoms C2 and C4. The $a_{H\alpha}$ values calculated with 6-31G(d) and with EPR-III for the radical decarboxylated differ by more than a factor of 2. The values obtained with 6-31G(d) are closer to the experimental ones, thus it appears that EPR-III basis set is not better for calculation of hfs constants than standard 6-31G(d).

4.2.2. Mechanisms for Asn degradation

The mechanisms of degradation induced by ionized radiations are poorly known. The preceding experimental

Table 4
Experimental and theoretical coupling constants and spin densities

Environment →	Exper. EPR	Vacuum		Water (ε=78)			Ethanol (ε=24)	
Entity ↓	a_H (G)	Spin density	a_H (G) 6-31G*	Spin density	a_H (G) 6-31G*	a_H (G) EPR-III	Spin density	a_H (G) 6-31G*
Asn radical cation							C2 0.35	
				O5 0.63			**O5 0.18**	
				O9 0.32			**O6 0.29**	
							O9 0.16	
Asn radical cation deprotonated		N1 0.52						
				O5 0.65			**O5 0.66**	
				O6 0.14			**O6 0.14**	
		O9 0.40		**O9 0.25**			**O9 0.24**	
Asn radical without H on C2		N1 0.23						
		C2 0.52		**C2 0.90**			**C2 0.92**	
		O6 0.18						
Asn radical without H on C4	H_α 15	**C4 0.93**	H_α 22	**C4 0.88**	H_α 21	H_α 20	**C4 0.93**	H_α 21
		O9 0.15						
Asn radical decarboxylated	H_α 21	N1 0.15	H_α 14		H_α 24	H_α 11		H_α 24
		C2 0.86		**C2 1.0**			**C2 1.0**	
Asn radical deamidated	H_α 22		H_α 24,25		H_α 21,24	H_α 21,22		H_α 22,25
		C4 1.0		**C4 1.0**			**C4 1.0**	
Asp radical cation deprotonated		**N1 0.71**		**N1 0.30**			**N1 0.29**	
		O9 0.14		**C2 0.34**			**C2 0.35**	
				C3 0.12			**C3 0.11**	
				O5 0.13			**O5 0.13**	
				O6 0.11			**O6 0.11**	
Asp radical anion		C3 0.36						
		O6 0.15						
		C7 0.25		**C7 0.56**			**C7 0.49**	
		O9 0.13		**O9 0.25**			**O9 0.25**	
Asp radical without H on C2		N1 0.25						
		C2 0.54		**C2 0.93**			**C2 0.93**	
		06 0.16						
Asp radical without H on C4	H_α 15	**C4 0.84**	H_α 20	**C4 0.81**	H_α 19	H_α 18	**C4 0.81**	H_α 20
		O9 0.17		**O9 0.18**			**O9 0.18**	
Asp radical decarboxylated at C2	H_α 21		H_α 14		H_α 24	H_α 22		H_α 25
		N1 0.15						
		C2 0.86		**C2 1.0**			**C2 1.0**	
Asp decarboxylated at C4	H_α 22		H_α 23,25		H_α 23,25	H_α 22,23		H_α 23,25
		C4 1.0		**C4 1.0**			**C4 1.0**	

In bold, spin densities on the same atoms in each environment.

results can be rationalized by the mechanisms proposed in Schemes 1 (electron ejection form Asn) and 2 (electron addition to Asn).

Although it is not observed experimentally, direct ionization of the Asn molecule should lead to the asparagine radical cation ($Asn^{\bullet+}$). Calculations indicate that ionization induces spin density on oxygen atoms located in the carboxyl group and in the amide group (Table 4). This result might indicate formation of two asparagine radical cations $Asn2(COO)^{\bullet+}$ (Scheme 1, reaction 1a) and $Asn2(CONH_2)^{\bullet+}$ (Scheme 1, reaction 2a). The $Asn2(COO)^{\bullet+}$ seems to be a precursor of decarboxylated radical $Asn(^{\bullet}CH)$ (Scheme 1, reaction 3) based on calculations showing elongation of the C2–C3 bond in the radical cation. Indeed, the $Asn(^{\bullet}CH)$ was observed in the EPR spectrum recorded at and above 250 K and CO_2 was detected in irradiated samples. Moreover, taking the respective energies from Table 1, one can easily calculate that decarboxylation process of the $Asn^{\bullet+}$ is exoenergetic ($\Delta E = -20.5$ kJ mol^{-1} in water). Another source of decarboxylated radical might be a concerted mechanism involving Asn1 conformation with a direct loss of CO_2 upon ionization (Scheme 1, reaction 1b). However, the lack of decarboxylated radicals in the EPR spectrum recorded at low temperatures suggests negligible contribution of reaction 1b involving the Asn1 conformer in polycrystalline asparagine. The $Asn2(CONH_2)^{\bullet+}$ might be a precursor of deamidated radicals $Asn(^{\bullet}CH_2)$ (Scheme 1, reaction 4). Formation of deamidation radicals was again confirmed in the EPR spectra recorded at and above 273 K. BDE calculations indicate that direct C4–C7 bond cleavage is energetically favourable (Table 2). However, structural changes do not involve the C4–C7 bond elongation in the radical cation. Therefore, reaction 4 seems to be of no importance in formation of deamidated radicals at low temperatures. However, an appearance of deamidation radicals at higher temperatures suggests that C4–C7 bond cleavage needs activation energy. Moreover, EPR spectra at low temperatures show no evidence of direct deamidation which speaks against concerted mechanism (Scheme 1, reaction 2b). Conversely the asparagine radical anion ($Asn^{\bullet-}$) is observed at

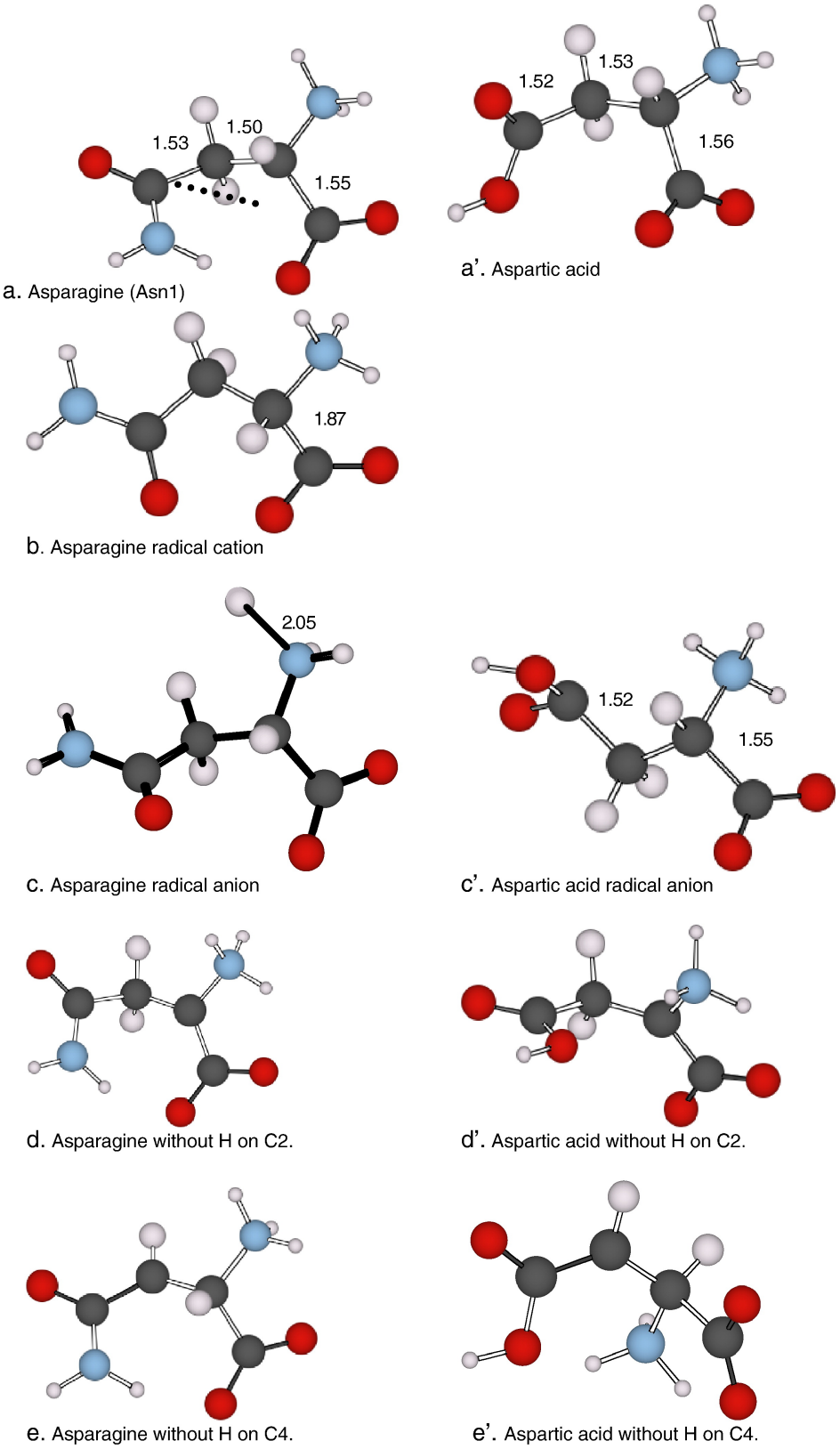

Fig. 3. Optimised structures of Asn and Asp and some derived radicals.

low temperature (77 K) by a doublet in the EPR spectrum. Nevertheless, calculations indicate that the $Asn^{\bullet -}$ is unstable and loses H atom from the amine group in a concerted mechanism (Scheme 2, reaction 5). There is no evidence in the EPR spectrum as well as in calculation results that the decay of the $Asn^{\bullet -}$ is accompanied by a simultaneous formation of

deaminated radicals. To our best knowledge, this is the first time that reaction 5 is proposed to rationalize instability of the $Asn^{\bullet -}$.

Another interesting feature (doublet of doublets observed in EPR spectra recorded at low temperatures starting at 150 K) was assigned to formation of the H-abstraction radical from the carbon atom C4 in a side chain of Asn. In amino acids, in general, H-abstraction radicals manifest in the EPR spectrum at much higher temperatures (nearly 273 K) as a result of hydrogen abstraction from the parent molecules by earlier formed decarboxylated or deaminated radicals [26]. An observation of the H-abstraction radical at the carbon atom C4 at very low temperatures after completion of the $Asn^{\bullet -}$ decay and before an appearance of decarboxylation and deamidation radicals suggests that highly mobile H atoms formed in reaction 5 might abstract a hydrogen atom from the asparagine at the carbon atom C4 (Scheme 2, reaction 6a). Another source for the H-abstraction radicals at the carbon atom C4 might be a hydrogen abstraction from the asparagine anion ($Asn^{\bullet -}$) formed simultaneously with hydrogen atom within a cage (Scheme 2, reaction 7a). It is quite surprising that there is no indication of the formation of the H-abstraction radicals at the carbon C2 at low temperatures via reactions 6b and 7b (Scheme 2). Bond dissociation energies calculated for both C–H bonds (Table 2) are similar around 420 kJ mol^{-1} in a zwitterionic form in water) and in the asparagine anion (around 400 kJ mol^{-1}). ΔE values for formation of H-abstraction radicals at C4 and C2 carbon atoms are calculated

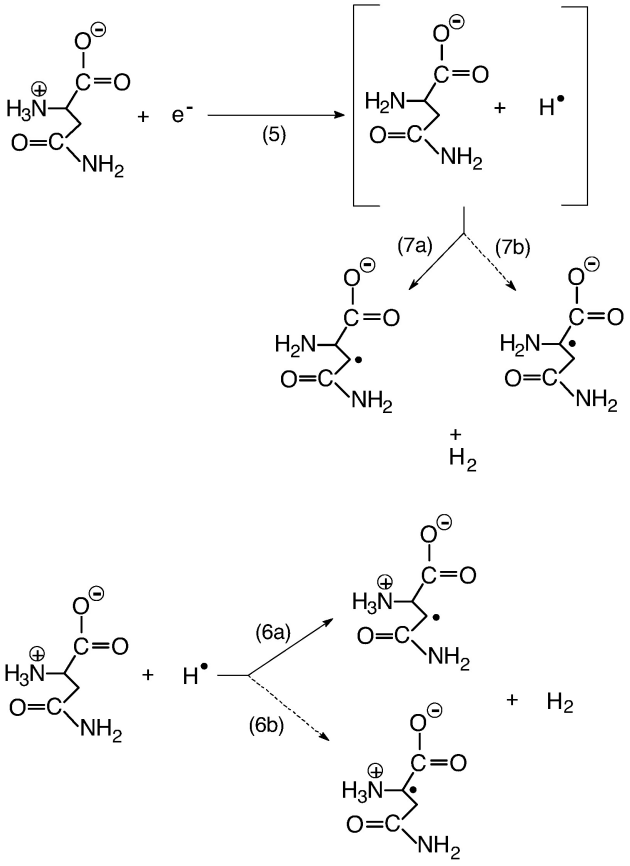

Scheme 2.

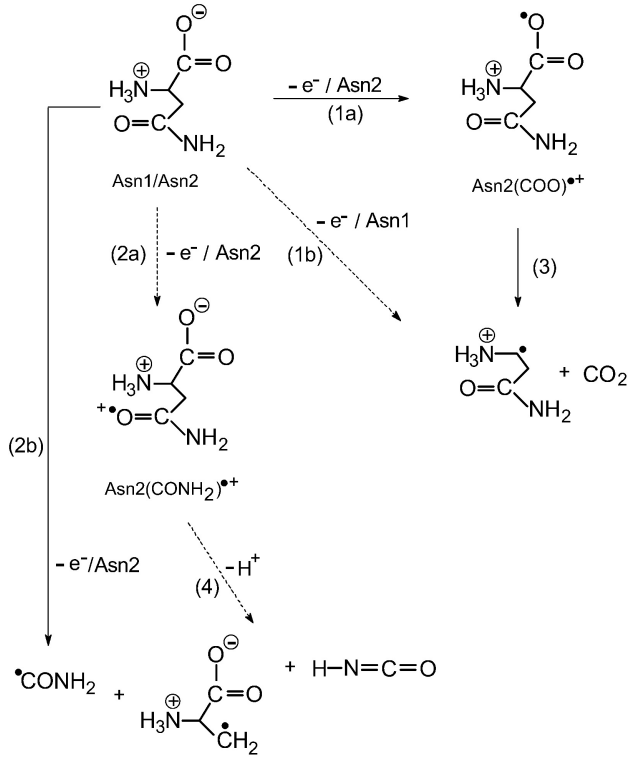

Scheme 1.

according to Eqs. (1) and (2), respectively and assuming their formation via direct hydrogen abstraction from the parent asparagine molecule by a hydrogen atom (Table 5). One has to note that both abstraction processes are characterised by ΔE similar values.

$$\Delta E_1 = [E(\mathrm{Asn(C4{-}H)}) + E(\mathrm{H_2})] - [E(\mathrm{Asn}) + E(\mathrm{H})] \quad (1)$$

$$\Delta E_2 = [E(\mathrm{Asn(C2{-}H)}) + E(\mathrm{H_2})] - [E(\mathrm{Asn}) + E(\mathrm{H})] \quad (2)$$

The lack of observation of H-abstraction radical at C2 carbon atom in EPR spectrum at high temperatures might be due to the complexity of the EPR spectrum. However, its formation at higher temperatures cannot be excluded.

Table 5
Hydrogen abstraction reaction energies in Asparagine (Asn) and Aspartic acid (Asp)

Environment →	Zwitterions in water (ε=78)	Zwitterions in ethanol (ε=24)	Anion in water (ε=78)
Reaction ↓	ΔE (kJ mol^{-1})	ΔE (kJ mol^{-1})	ΔE (kJ mol^{-1})
H+Asn→H_2+Asn(C2–H)	−44.7	−47.7	−78.4
H+Asn→H_2+Asn(C4–H)	−56.9	−69.1	−58.2
H+Asp→H_2+Asp(C2–H)	−36.3	−46.5	
H+Asp→H_2+Asp(C4–H)	−48.3	−60.0	

4.3. Aspartic acid

4.3.1. Experimental EPR results

In aspartic acid at 77–95 K, EPR signal is characterized by a broad singlet with $g=2.003$, and a width $\Delta H=12$ G. This singlet is assigned to the aspartic acid radical anion formed by an addition of electron to a carboxyl group (Fig. 4, top). However, in single crystals Ogawa found a doublet that he interpreted as coming from electron addition on the carboxylate group [32]. At 120 K a pure doublet of doublets was observed with the hyperfine splittings of $a_{H\alpha}=15$ G and $a_{H\beta}=3.5$ G and $g=2.003$ (Fig. 4, middle), and assigned to the hydrogen abstraction radical from the methylene group (C4) in the side chain of aspartic acid. A spectrum with similar features and the same hyperfine splittings was observed in asparagine (*vide supra*). Starting at 150 K, an additional weak signal was observed whose intensity increases on further warming to about 250 K. This new multiline signal was resolved into two components: previously observed the doublet of doublets and a four line component with $a_{H\alpha}=21$ G and $a_{H\beta}=23$ G. These isotropic values are in agreement with those of Ogawa et al. [32]. The latter component was assigned to the aspartic acid decarboxylated radical at C2 position. However, in single crystals Ogawa reported similar EPR spectrum attributed to deaminated radical in addition to dehydrogenated radical on C2 [32]. As the temperature was increased to 273 K, the spectrum in aspartic acid indicated the presence of three radical species as for Asn (Fig. 4, bottom). This spectrum can also be simulated by previously recorded at lower temperatures a four line component with $a_{H\alpha}=21$ G and $a_{H\beta}=23$ G (30%), a doublet of doublets with $a_{H\alpha}=15$ G and $a_{H\beta}=3.5$ G (30%) and by a new wide multiline component with $a_{H\alpha}=22$ G and $a_{H\beta}=42$ G (40%). The multiline component was assigned to the decarboxylated radical from the side chain of aspartic acid. These radicals are still stable at room temperature.

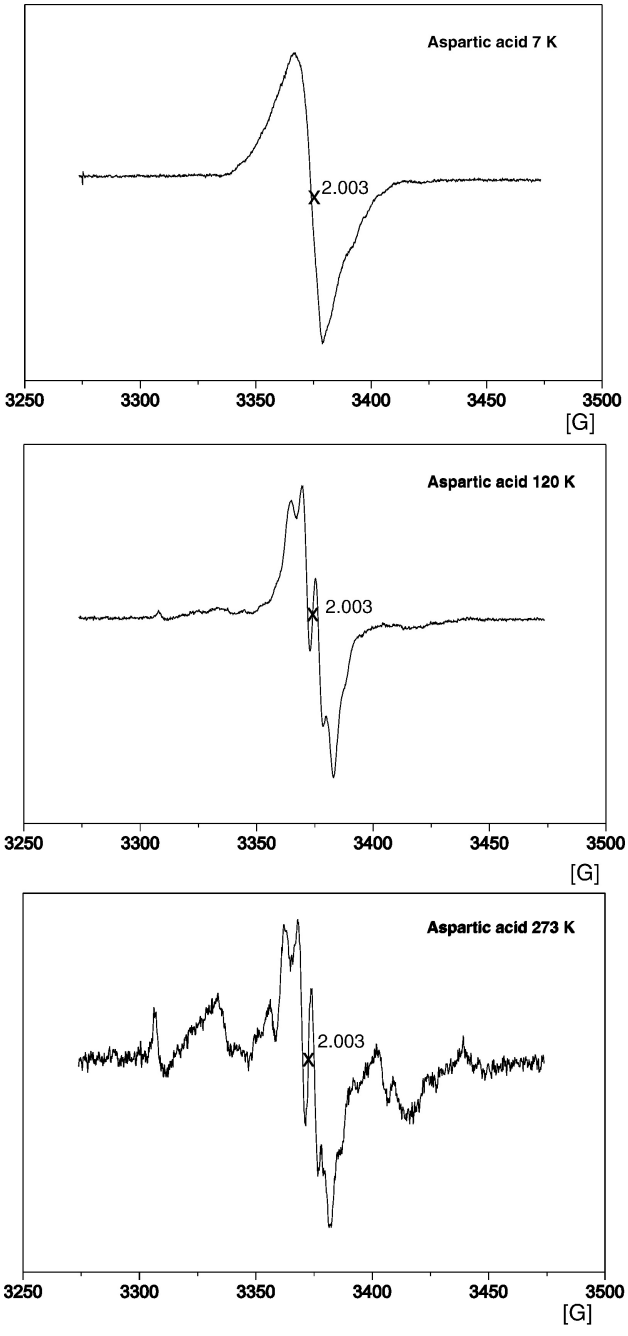

Fig. 4. Experimental EPR spectra recorded at 77 K (top), 120 K (middle), and 273 K (bottom) in aspartic acid irradiated at 77 K.

4.4. CO_2 measurements

Additional support for the existence of decarboxylated radicals in asparagine and aspartic acid was obtained by carbon dioxide analysis in irradiated samples. The calculated yields of the CO_2 formation (expressed in G-units/100 eV of energy) are: 0.5 and 1.6 for asparagine and for aspartic acid, respectively.

4.4.1. Structures, energies and charge distributions

As expected, there is no cyclisation by intramolecular hydrogen bond for Asp and therefore only one stable conformation was found (Fig. 3, structure a′). As far as the radical cation derived from Asp is concerned it could not be optimized unless the amine function is deprotonated. In deprotonated radical cation the C2–C3 bond was strongly elongated (by 0.5 Å). On the other hand, it is interesting to note that the C4–C7 bond does not change significantly upon oxidation. These data suggest that electron ejection that leads to the stable deprotonated form of radical cation is followed by the decarboxylation pathway involving mainly the carboxylic group located at the C2 with a small contribution, if any, of the carboxylic group located at the C4. Conversely, radical anion has a stable structure. It exhibits only conformational changes, however, without bond length modifications compared to the parent molecule (Fig. 3, structure c′).

The respective energies of the deprotonated radical cation and the radical anion calculated for various environments are reported in Table 6. Ionization potential of the zwitterion is much lower (4.5 eV in water and ethanol) and is slightly higher (8.4 eV) in the vacuum in comparison to the respective values for Asn (*vide supra*). Electronic affinity is sensitive to the

Table 6
Energies of Aspartic acid and radicals derived from Asp

Environment →	Zwitterions in water (ε=78)	Zwitterions in ethanol (ε=24)	Vacuum
Entity ↓	*E* (a.u.)	*E* (a.u.)	*E* (a.u.)
Asp	−512.33763	−512.32996	−512.29960
Asp radical cation	[a]	[a]	
Asp radical cation deprotonated	−511.67660	−511.68565	−511.99116
Asp radical anion	−512.36337	−512.43122	−512.25196
Asp without H on C2	−511.67375	−511.67069	−511.67952
Asp without H on C4	−511.67835	−511.67585	−511.64622
H	−0.49790	−0.498611	−0.50027
Asp decarboxylated at C2	−323.10213	−323.10133	−323.09107
Asp decarboxylated at C4	−323.08521	−323.08440	−323.06488
CO_2	−188.58030	−188.58451	−188.58094

[a] Not stable.

environment (0.7, 2.8, and 1.3 eV in water, ethanol and the vacuum, respectively).

Both hydrogen abstraction processes from the carbon atoms C2 and C4 result in alkyl radicals quasi isoenergetic (Table 6) and with very similar structures (Fig. 3, structures d′ and e′). In CCl_4 it induces proton transfer from the NH_3^+ to COO^- leading to the neutral species as in vacuum. Similarly as for Asn, the BDE in vacuum is lower for the hydrogen abstraction from C2 and they are again not much sensitive to the environment and hydrogen abstracted (ranged from 400 to 460 kJ mol^{-1}) (Table 2). Bond dissociation energies of C2–C3 and C4–C7 bonds are quasi equivalent with BDE around 520–560 kJ mol^{-1} except for both BDEs in the vacuum that are lower (Table 2). One has also to note that all respective BDE values in Asp are higher in comparison to Asn.

Changes in the Mulliken charge distribution after oxidation or electron attachment involve mainly oxygen atoms in carboxylic groups (Table 3). For the deprotonated aspartic acid radical cation a change in the negative charge distribution occurs mainly on the oxygen atoms located in the carboxyl group linked to C2 (α-carbon). For the radical anion a change in the negative charge distribution occurs mainly on the oxygen atoms located in the carboxyl group linked to C4 (side chain). It is interesting to note that hydrogen abstraction does not affect charge distribution in radicals formed.

4.4.2. Coupling constants and spin densities

A fairly good agreement was found between experimentally measured and calculated $a_{H\alpha}$ values for both decarboxylation radicals derived from aspartic acid in zwitterionic forms (in water, ethanol and CCl_4) (Table 4). Discrepancy noted between experimentally measured and calculated $a_{H\alpha}$ values for decarboxylation radicals in vacuum confirms also that the amine group in these radicals is protonated. As far as H-abstraction radicals from the carbon atom C4 are concerned, the calculated $a_{H\alpha}$ values are higher from those observed experimentally.

Since the protonated radical cation of aspartic acid is not stable all spin densities are given for its deprotonated form. It is interesting to note that in all environments spin density is distributed on the α-carbon C2, the carboxyl group attached to it, and on the nitrogen atom. The spin density distribution is slightly different in comparison to Asn radical cation where it is only spread over oxygen atoms. However, it is significantly different in deprotonated radical cation in the vacuum. It mainly involves the nitrogen and oxygen atom in the carboxyl group located in a side chain of aspartic acid. In water, spin density distribution in the aspartic acid radical anion involves only the carbon and the oxygen atom in the carboxyl group located in a side chain. It is worthy to note that in the vacuum, spin density distribution involves additionally the carbon and oxygen atom in the carboxyl group attached to the α-carbon.

Generally, the spin density in radical anions and cations are spread over several atoms. As far as the spin density in alkyl radicals is concerned it is localized on the respective carbon atoms.

4.4.3. Mechanisms of Asp degradation

In the case of Asp the electron addition leads to a stable anion, whereas electron ejection initiate more complex transformation than for Asn. We propose Schemes 3 and 4 to depict the fate of the radical cation from Asp.

Like in Asn, direct ionization of the Asp molecule to the radical cation ($Asp^{\bullet+}$) (Scheme 3, reaction 8a) is not observed. Indeed, according to calculations the radical cation cannot be optimized with protonated amine group of Asp. We propose instead that ionization is accompanied by a net hydrogen atom

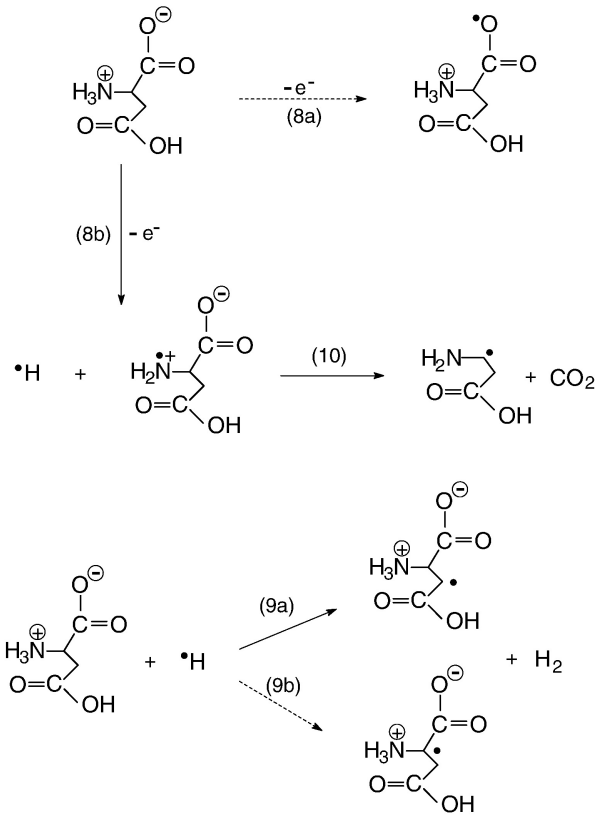

Scheme 3.

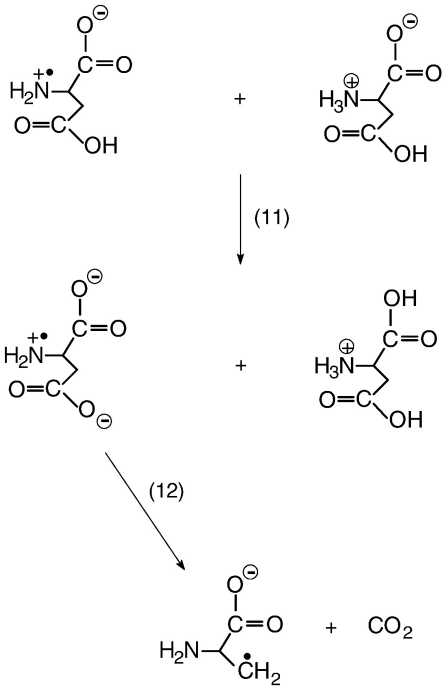

Scheme 4.

ejection (Scheme 3, reaction 8b). Due to its high mobility hydrogen atom might abstract another hydrogen from the methylene group located in the side chain of Asp (Scheme 3, reaction 9a). This is in agreement with EPR observation of the H-abstraction radicals at C4 at low temperatures. Like in Asn, it is quite surprising that there is no indication of the formation of the H-abstraction radicals at the carbon C2 at low temperatures via reaction 9b (Scheme 3). Bond dissociation energies calculated for both C–H bonds (Table 2) are similar around 440 kJ mol^{-1} in a zwitterionic form in water. ΔE values for formation of H-abstraction radicals at C4 and C2 carbon atoms are calculated according to Eqs. (3) and (4), respectively, and assuming their formation via direct hydrogen abstraction from the parent aspartic acid molecule by a hydrogen atom (Table 5). One has to note that both abstraction processes are characterised by similar ΔE values.

$$\Delta E_3 = [E(\mathrm{Asp(C4{-}H)}) + E(\mathrm{H_2})] - [E(\mathrm{Asp}) + E(\mathrm{H})] \quad (3)$$

$$\Delta E_4 = [E(\mathrm{Asp(C2{-}H)}) + E(\mathrm{H_2})] - [E(\mathrm{Asp}) + E(\mathrm{H})] \quad (4)$$

Again, the complexity of the EPR spectra at higher temperatures does not allow concluding about the presence of H-abstraction radicals at C2 carbon atom.

As a result of ionization, N-centered radical cation is formed in which C2–C3 bond is elongated. This should lead to decarboxylation at C2 (Scheme 3, reaction 10) what was confirmed by observation of the corresponding decarboxylated radical. Formation of the decarboxylated radical located at C4 might be rationalized taking into consideration the arrangement of molecules in the aspartic acid crystal [33]. It was shown that the carboxylic acid function is linked to the carboxylate moiety of another molecule by hydrogen bonding. Hence, an intermolecular proton transfer can take place between the radical cation of Asp and intact molecule (Scheme 4, reaction 11). The resulting radical cation with deprotonated carboxyl group at the side chain undergoes decarboxylation (Scheme 4, reaction 12). Indeed, the ease of decarboxylation at C2 and C4 is confirmed by similarity of BDE values of C2–C3 and C4–C7 bonds (Table 2).

An observation of a singlet in the EPR spectrum suggests the formation of the aspartic acid radical anion (Asp$^{\bullet -}$) at low temperatures. The stability of the radical anion was confirmed by calculations (Table 6 and Fig. 4, structure c′). This radical might undergo deamination; however, in the observed EPR spectrum, it is not possible to distinguish deaminated radicals from decarboxylated radicals at C2 position.

5. Conclusions

The radiation induced degradation processes of two amino acids, asparagine (Asn) and aspartic acid (Asp) were studied using EPR spectroscopy and by quantum mechanical calculations using DFT methods.

EPR spectra were obtained in the same experimental conditions for both amino-acids. The assignments of each band lead to observation of the evolution of the radical species over a wide range of temperature. It completes the previous results obtained on Asn and Asp by different authors. The identification of radicals and their evolution with the temperature allowed us to make hypotheses concerning the mechanisms of transformations of very short lived initial radical cations or anions. These mechanisms are supported by both EPR experimental results and quantum chemical calculations results.

To mimic the crystal in which both amino-acids are in the zwitterionic forms we considered a solvent environment with three dielectric constants, $\varepsilon = 2$ (CCl_4), 24 (ethanol) and 78 (water). The lowest value ($\varepsilon = 2$) is usually attributed to the proteic interiors and were found suitable in other quantum chemistry calculations about protein free radicals [34]. The highest one is characteristic of the aqueous medium, thus it gives information about what may happen in biological medium. As the crystal environment is not really described by dielectric constants we enlarged our simulation by performing also calculations with an intermediate value ($\varepsilon = 24$). Actually, the results are slightly sensitive to the dielectric constant. The energetical and coupling constants remain the same, thus the proposed mechanisms do not change with the medium. However we noted a destabilization of the zwitterionic forms with $\varepsilon = 2$, where the proton of NH_3^+ is transferred to the carboxylate group leading to the neutral species like in vacuum. Thus CCl_4 does not seem to be the most accurate model of the crystal because this proton transfer should not happen intramolecularly.

It is interesting to note that the behaviour of both amino acids is not the same although their chemical structures are very similar. Both radical anions are observed by EPR, however calculations show that Asn$^{\bullet -}$ is destabilized: attachment of an electron results in hydrogen loss from the amine group. As for radical cations from both amino acids, they are not observed by

EPR even at low temperatures. Calculations indicate that radical cation derived from Asn is a precursor of decarboxylated and deamidated radicals. In Asp ionization of the parent molecule leads to hydrogen loss from the amine group and consecutive decarboxylation of the N-centered radical cation. However the secondary reactions of hydrogen atoms with Asn and Asp parent molecules lead to similar H-abstraction radicals in the side chains.

Acknowledgments

Two of us (CHL and KB) are indebted to the COST P9 program for covering expenses for a trip to Poland and France, respectively.

We thank IDRIS (projects 020268 to 040268), ICM-UW (project G24-13).

References

[1] H.R. Stennike, G.S. Salvesen, Catalytic properties of the caspases, Cell Death Differ. 6 (1999) 1054–1059.
[2] D. Voet, J.G. Voet, Biochemistry, 2nd edition. Wiley & Sons, 1995.
[3] N.E. Robinson, A.B. Robinson, Deamidation of human proteins, Proc. Natl. Acad. Sci. 98 (2001) 12409–12414.
[4] A.R. Hipkiss, On the "struggle between chemistry and biology during ageing" implications for DNA repair, apoptosis and proteolysis, and a novel route of intervention, Biogerontology 2 (2001) 173–178.
[5] S. D'Angelo, D. Ingrosso, B. Perfetto, A. Baroni, M. Zappia, L.L. Lobianco, M. Tufano, P. Galetti, UVA irradiation induces L-isoaspartyl formation in melanoma cell proteins, Free Radic. Biol. Med. 31 (2001) 1–9.
[6] C.E.M. Voorter, W.A. de Haard, P.J.M. van den Oetelaar, H. Bloemendal, W.W. de Jong, Spontaneous peptide bond cleavage in aging α-crystalline through a succinimide intermediate, J. Biol. Chem. 263 (1988) 19020–19023.
[7] M. Stuart-Audette, Y. Blouquit, M. Faraggi, C. Sicard-Roselli, C. Houée-Levin, P. Jollès, Re-evaluation of intramolecular long-range electron transfer between tyrosine and tryptophan in lysozymes. Evidence for the participation of other residues, Eur. J. Biochem. 270 (2003) 3565–3571.
[8] B. Bambai, C.E. Rogge, B. Stec, R.J. Kulmacz, Role of Asn-382 and Thr-383 in activation and inactivation of human prostaglandin H synthase cyclooxygenase catalysis, J. Biol. Chem. 279 (2003) 4084–4092.
[9] M. Vijayakumar, H. Qian, H.X. Zhou, Hydrogen bonds between short polar side chains and peptides backbone: prevalence in proteins and effects on helix-forming propensities, Proteins 34 (1999) 497–507.
[10] A.P. Jonsson, T. Bergman, H. Jornval, W.J. Griffith, Gln-Gly cleavage: a dominant site in the fragmentation of protonated peptides, Rapid Commun. Mass Spectrom. 15 (2001) 713–720.
[11] H.J. Cooper, R.R. Hudgins, K. Hakanson, Marshall, Characterization of amino acid side chain losses in electron capture dissociation, J. Am. Soc. Mass Spectrom. 13 (2002) 241–249.
[12] A. Filali-Mouhim, M. Audette, M. St Louis, L. Thauvette, L. Denoroy, F. Penin, X. Chen, N. Rouleau, J.-P. Le Caer, J. Rossier, M. Potier, M. Le Maire, Lysozyme fragmentation induced by gamma-radiolysis, Int. J. Radiat. Biol. 72 (1997) 63–70.
[13] H. Shields, W. Gordy, Electron spin resonance studies of radiation damage to amino acids, J. Phys. Chem. 62 (1958) 789–798.
[14] D. Duling, WinSIM 2003, http://epr.niehs.nih.gov/pest_mans/winsim.html.
[15] M.J. Frisch, G.W. Trucks, H.B. Schlegel, G.E. Scuseria, M.A. Robb, J.R. Cheeseman, V.G. Zakrzewski, J.A. Montgomery Jr., R.E. Stratmann, J.C. Burant, S. Dapprich, J.M. Millam, A.D. Daniels, K.N. Kudin, M.C. Strain, O. Farkas, J. Tomasi, V. Barone, M. Cossi, R. Cammi, B. Mennucci, C. Pomelli, C. Adamo, S. Clifford, J. Ochterski, G.A. Petersson, P.Y. Ayala, Q. Cui, K. Morokuma, D.K. Malick, A.D. Rabuck, K. Raghavachari, J. Cioslowski, J.V. Ortiz, A.G. Baboul, B.B. Stefanov, G. Liu, A. Liashenko, P. Piskorz, I. Komoromi, R. Gomperts, R.L. Martin, D.J. Fox, T. Keith, M. A. Al-Laham, C.Y. Peng, A. Nanayakkara, C. Gonzalez, M. Challacombe, P.M.W. Gill, B. Johnson, W. Chen, M.W. Wong, J.L. Andres, M. Head-Gordon, E.S. Replogle, J.A. Pople, Gausian, vol. 03, Gaussian Inc., Pittsburgh, PA, 2003, Rev. B.03.
[16] B. Braïda, P.C. Hiberty, A.J. Savin, A systematic failing of current density functionals: overestimation of two-center three-electron bonding energies, J. Phys. Chem., A 102 (1998) 7872–7877.
[17] J. Bergès, F. Fuster, J.-P. Jacqout, C. Silvi, C. Houée-Levin, Influence of protonation on the stability of disulfide radicals, Nukleonika 45 (2000) 17–22.
[18] S. Carles, C. Desfrancois, J.P. Schermann, J. Bergès, C. Houée-Levin, Rydberg electron transfer spectroscopy and ab-initio studies of dimethyl sulfoxide-water neutral and anion dimers, Int. J. Mass Spectrom. 205 (2001) 227–232.
[19] C. Houée-Levin, J. Bergès, A DFT study of electron and hole localisation in a peptide containing asparagine, Eur. J. Phys., D 20 (2002) 551–555.
[20] A. Rauk, D.A. Armstrong, J. Bergès, Glutathione radical: intramolecular H abstraction by the thiyl radical, Can. J. Chem. 79 (2001) 405–417.
[21] X. Li, Z. Cai, M.D. Sevilla, DFT calculations of the electron affinities of nucleic acid bases: dealing with negative electron affinities, J. Phys. Chem., A 106 (2002) 1596–1603.
[22] M. Cossi, V. Barone, B. Mennucci, J. Tomasi, Ab initio study of ionic solutions by a polarizable continuum dielectric model, Chem. Phys. Lett. 286 (1998) 253–260.
[23] M. Cossi, C. Adamo, V. Barone, Solvent effects on the profile of an SN2 reaction, Chem. Phys. Lett. 297 (1998) 1–7.
[24] M.L. McKee, Comparison of gas-phase and solution-phase reactions of dimethyl sulfide (DMS) and 2-(methylthio)ethanol (2-MTE) with hydroxyl radical, J. Phys. Chem., A 107 (2003) 6819–6827.
[25] N. Rega, M. Cossi, V. Barone, Development and validation of reliable quantum mechanical approaches for the study of free radicals in solution, J. Chem. Phys. 105 (1996) 11060–11067.
[26] M. Sevilla, Radicals formed by the reaction of electrons with amino acids in an alkaline glass, J. Phys. Chem. 74 (1970) 2096–2102.
[27] H.C. Box, H.G. Freund, K.T. Lilga, E.E. Budzinski, Hyperfine couplings in primary radiation products, J. Chem. Phys. 63 (1975) 2059–2063.
[28] J. Sinclair, P. Codella, Radiation damage produced in single crystals of *N*-acetylglycine, J. Chem. Phys. 59 (1973) 1569–1576.
[29] D.M. Close, G.W. Fouse, W.A. Bernhard, ESR and ENDOR study of single crystals of L-asparagine·H_2O X-irradiated at room temperature, J. Chem. Phys. 66 (1977) 1534–1540.
[30] M. Ramanadham, S.K. Sikka, R. Chidambaram, Structure of L-asparagine monohydrate by neutron diffraction, Acta Crystallogr., B 28 (1972) 3000–3005.
[31] J.J. Verbist, M.S. Lehmann, T.F. Koetzle, W.C. Hamilton, Precision neutron diffraction structure determination of protein and nucleic acid components: VI. The crystal and molecular structure of the amino acid L-asparagine monohydrate, Acta Crystallogr., B 28 (1972) 3006–3010.
[32] M. Ogawa, K. Ishigure, K. Oshima, ESR study of irradiated single crystals of amino acids: II. L-Aspartic acid, Radiat. Phys. Chem. 16 (1980) 289–294.
[33] J.L. Derissen, H.J. Endeman, A.F. Peerdeman, The crystal and molecular structure of L-aspartic acid, Acta Crystallogr., B 24 (1968) 1349–1354.
[34] J. Bergès, E. Kassab, D. Conte, E. Adjadj, C. Houée-Levin, Ab initio calculations on arginine–disulfide complexes modelling the one-electron reduction of lysozyme, J. Phys. Chem. 101 (1997) 7809–7817.